Retinoid X Receptor as a Novel Drug Target to Treat Neurological Disorders Associated with α-Synucleinopathies.

Assylbek Zhylkibayev[1,2], Christopher R. Starr[1,3], Venkatram Atigadda [1,3], Maria B. Grant [1,4], Marina S. Gorbatyuk [1,2,5*], and Oleg S. Gorbatyuk[1,2,6*].

[1] University of Alabama at Birmingham, [2]Department of Optometry and Vision Science, [3]Department of Dermatology, [4]Department of Ophthalmology, [5]Neuroscience Center, [6]Department of Neurology, Center for Neurodegeneration and Experimental Therapy.

* To whom correspondence should be addressed:

Oleg Gorbatyuk: oleggor@uab.edu

Marina Gorbatyuk: mgortk@uab.edu

Abstract

The pathology of Parkinson's Disease (PD) is multifaceted, with chronic neuroinflammation associated with glial cell activation standing out as a hallmark of PD pathophysiology. While a few treatments exist to interfere with inflammation, a breakthrough therapy based on innovative molecular mechanisms and targets is still awaited. The nuclear retinoid X receptor (RXR) is of particular interest for therapeutic intervention due to its ability to bind and activate permissive partners, NURR1 and PPARs, which have been shown to be dysfunctional in PD brains. Therefore, the goal of this study was to validate RXR-based therapy to slow down PD pathogenesis. Adult C57BL6 male mice were used in the study. PD-like pathology was triggered by co-delivery of AAV expressing α-Syn and PFF (AAV/PFF) to the substantia nigra pars compacta. The therapeutic potential of RXR activation was evaluated using AAV-mediated gene transport. Unbiased stereology, immunohistochemical analysis, LC/MS, and western blotting were employed to assess the therapeutic effect. At 8 weeks post-injection—elevated GFAP and Iba1 levels, associated with accumulated LB-like aggregates, pronounced loss of TH neuronal cells, and diminished dopamine (DA) levels—were observed in affected brains. Moreover, PPAR and NURR1 protein levels were also reduced in these brains. Conversely, RXR overexpression resulted in an increase in PPAR and NURR1 levels, a reduction in GFAP and Iba1 levels, and a decrease in the number and distribution of LB-like aggregates. These phenomena were also accompanied by the prevention of tyrosine hydroxylase $(TH)^+$ cell loss and the DA deficit in the treated brains. Therefore, our data provide direct evidence of the therapeutic potential of RXR-based therapy and highlight RXR as a novel drug target for PD.

Introduction

Alpha-synucleinopathies (α-SNP) including Parkinson's disease (PD) and dementia with Lewy bodies (LB) rank as the most prevalent neurodegenerative condition after Alzheimer's disease (AD), characterized by abnormal intraneuronal inclusions of α-synuclein (αS). While the pathology of PD is multifaceted—involving several interconnected processes, including the degeneration of dopamine (DA) nigral neurons, LB formation, mitochondrial dysfunction, protein aggregation, impaired clearance, and oxidative stress—chronic neuroinflammation stands out as a hallmark of PD pathophysiology. The glial cell activation and heightened levels of pro-inflammatory factors constitute prevalent features of the PD-afflicted brain.[1] To date, while a few treatments exist to interfere with inflammation and immune deficiency, including minocycline, dexamethasone, and several non-steroid anti-inflammatory drugs protecting DA neurons from degeneration and glial cell activation, a breakthrough therapy based on innovative molecular mechanisms and targets is urgently required.

The modulation of nuclear receptors (NRs) has been proposed as one of the most attractive therapeutic strategies for correcting PD pathobiology.[2-8] The nuclear retinoid X receptor (RXR) is of particular interest for therapeutic intervention, due to its binding and activation of both permissive partners, NURR1 and PPARs, whose dysfunctions have been observed in AD, multiple-system atrophy (MS), and PD[9-11] and which are known to regulate the expressions of inflammation-associated genes.[12, 13] Despite the importance of pharmacological RXR activation against PD-causing toxins,[2, 14, 15] effective RXR-based treatments for PD patients are still in development.

Cumulative evidence indicates that abnormal RXR signaling affects neuronal stress and neuroinflammation in PD pathobiology.[3, 5] Furthermore, the activation of RXR binding partners, either NURR1 or PPAR, is beneficial for reversing the PD pathology seen in animal and cellular models of PD.[2, 4, 8, 12, 16-18]. Moreover, the published studies have shown that the activation of RXR by treatment with RXR ligand LG100268 protects DA neurons from stress and PD-like pathology [3], PPAR by the treatment with PPAR agonists fenofibrate and GW501516 reduce neuroinflammation and PD neurodegeneration[12], and the activation of the NURR1/RXRα heterodimer by NURR1 agonists can stand as a monotherapy for PD to increase striatal DA levels and up-regulate NURR1 target genes in PD-like brain conditions.[19] Therefore, we were keen to learn whether destabilized RXR/PPAR and RXR/NURR1 complexes contribute to PD pathogenesis via a dysregulated immune response and whether treatment of the PD brain with overproduced exogenous RXR enhances the pool of RXR homodimers available to partner with PPARs and/or NURR1, providing an effective intervention aimed at controlling inflammatory response and reversing PD pathobiology.

Using recombinant adeno-associate virus (AAV) to overexpress human RXRα (AAV-RXR) in the mouse substantia nigra pars compacta (SNc), in the present study, we examined the role of RXR in PD pathogenesis. Specifically, we investigated the impact of RXR on the inflammatory response and the viability of nigral tyrosine

hydroxylase positive (TH^+) cells. We proposed the RXR-based therapy as a novel treatment to reduce pathobiological events in the PD-affected brains and to slow down the disease progression.

Methods

Animals. The study was conducted according to the UAB IACUC protocol #10085. In our study, we employed an animal model of PD-like pathology recently described by Bjorklund A et al.[20] C57BL6 adult male mice were used in the study. In order to mimic the PD pathogenesis, we used combined injections of rAAV-αS and α-S Preformed Fibrils (αS-PFF) purchased from Stressmarq (SPR-322) in the SNc. The αS-PFFs were used at a concentration of 5 mg/ml. The rAAV containing a blank expression cassette (BV), which is an αS vector with an early stop codon, was employed as a control virus.[21, 22] Monomeric αS (Stressmarq; SPR-321)was used as a control substance to αS-PFF. A mixture of BV and monomeric αS (BV/αS) served as a control for combined AAV/PFF administration. Mice were injected with the AAV/PFF or BV/αS mixtures on one side of the brain; the other side was kept as a non-transduced control.

AAV vectors. All vectors have been packaged in AAV2/5 capsid and purified as described previously.[22] Titers for all AAV constructs were equalized to 6 $x10^{12}$ vg/ml.

Intracerebral injection of αS-PFF and rAAV vectors. All surgical procedures were performed using aseptic techniques and isoflurane gas anesthesia as previously described. [23] Stereotaxic coordinates for intranigral injections in C57BL6 mice (two-month-old males, 28±3 g) are AP -2.9 mm, ML +1.3 mm, and DV -4.1 mm, relative to the bregma. The total injection volume is 1.0 µl or 1.5 µl at a speed of 0.5 µl/min. For these injections, we used a pulled glass pipet with an outer diameter not exceeding 40–45 µm to avoid needle-related damage and reduce the injury-mediated inflammatory response.

Isolation and Processing of Tissues. Animals were deeply anesthetized by ketamine (50 mg/kg) and xylazine (10 mg/kg) cocktail intraperitoneally. Brains were removed and divided into two parts. The caudal part containing the SNc was fixed in ice-cold 4% paraformaldehyde in 0.1 M phosphate buffer (PB), pH 7.4. The fixed part of the brains was stored overnight at 4°C and then transferred into 30% sucrose in 0.1 M PB for cryoprotection. Thirty µm thick coronal sections were cut and processed for immunohistochemistry. The rostral piece of brain tissue was used immediately to dissect the right and left striatum. Tissue samples were frozen separately on dry ice and kept at -80ºC until assayed. Mice from the 4-week time point were used to obtain SNc tissue samples for Western blot analysis. Frozen brains were sectioned on a Leica CM1510S cryostat (Leica, Buffalo Grove, IL, USA) into 150 µm slices with SNc tissue subsequently dissected out under a microscope as described previously.[22]

Immunohistochemistry. For the bright-field microscopy analysis, 30µm floating sections were preincubated with 1% H2O2–10% methanol for 15 min and then with 5% normal goat serum for 1 h. Sections were incubated overnight at room temperature with anti-TH (1:2000; #MAB318, mouse; Millipore) antibody. Next, incubation with biotinylated secondary anti-mouse antibody was followed by incubation with avidin–biotin–peroxidase complex (VECTASTAIN® Elite® ABC-HRP Kit, Peroxidase (Standard) (PK-6100) Vector Laboratories, Burlingame, CA, USA). Reactions were visualized using NovaRED Peroxidase (HRP) Substrate

Kit (Vector NovaRED® Substrate Kit, Peroxidase (HRP) (SK-4800), Vector Laboratories, Burlingame, CA, USA).

For confocal microscopy, sections were incubated with primary antibodies against human αS (1:1000; 32-8100, mouse; Invitrogen), α-phospho-Serine129 (pS129) (Recombinant Anti-Alpha-synuclein (phospho S129) antibody [EP1536Y] (ab51253); 1:500; ab51253, rabbit mAb; Abcam), TH (Anti-Tyrosine Hydroxylase Antibody; 1:1000; AB1542, sheep; Millipore), human RXRα (RXRA Monoclonal Antibody (K8508); 1:200; 43-390-0; mouse ~~rabbit~~; Invitrogen), and secondary fluorescent antibodies labeled with Alexa Fluor 488, 555, and 647 (1:500 for all; PIA32773-mouse; A21202-mouse; PIA32731TR-rabbit; PIA32794-rabbit; A21448-sheep, Invitrogen). The sections were examined using an AX-R Confocal Microscope coupled to a fully automated Ti2-E system (Nikon Instruments Inc. Melville, NY, USA). NIS-Elements Software package was used for post-capture image analysis. Sequential scanning was used to suppress optical crosstalk between the fluorophores in stationary-structure colocalization assays. All manipulations of contrast and illumination on color images as well as color replacement were made using Adobe Photoshop CS software (Version 23.5.5).

Quantitation of Phospho-Synuclein Aggregates. To quantify phosphor-synuclein aggregates, 30μm floating brain sections were processed for immunofluorescent labeling with pS129 antibody. To count pS129-positive aggregates, an ImageJ macro was developed by modifying a previously described macro designed for automated cell counting.[24] Briefly, the parameters of the counter were adjusted to reliably count aggregates. There was a strong agreement between macro-counted sections and those counted manually. To count the aggregates in the macro, an area of interest was drawn on a micrograph within ImageJ and then the macro was run in order to count the total number of aggregates in the outlined area. The area occupied by aggregates was manually quantified in ImageJ using the freehand tool and the measure function.

Unbiased Stereology. The unbiased stereological estimation of the total number of the TH+ neurons in SNc was performed using the optical fractionator method as described previously.[25] The sampling of cells to be counted was performed using the MicroBrightfield StereoInvestigator System. The software was used to delineate the transduction area at 4x on 30 μm sections and generate counting areas of 100 x 100 μm. The estimate of the total number of neurons and coefficient of error due to the estimation was calculated according to the optical fractionator formula. [25]

DA measurements. Frozen striatal tissue samples were shipped on dry ice to the Neurochemistry Core Lab at Vanderbilt University Medical Center, Nashville, TN for HPLC analysis of dopamine (DA), 3,4-dihydroxyphenylacetic acid (DOPAC), and homovanillic acid (HVA) in the striatum. A total of 5-6 animals were analyzed for striatal DA metabolites per group.

Immunoblotting (Western blotting) Analysis. Brain tissues were collected and lysed with RIPA buffer (Cell signaling, 9806, USA) supplemented with 1% Halt Protease and phosphatase inhibitor cocktail (Thermo Fisher Scientific, 87786, USA). Samples were homogenized using a pestle (Fisherbrand™ RNase-Free Disposable Pellet Pestles; 12-141-368; Fisher, USA) and rotated at 4°C for 30 min, and centrifuged at 4°C by 12000g speed for 15 min. Based on the Bradford method, the supernatant was used for protein quantitation using a

protein assay (Bio-Rad Protein Assay Kit I; 5000001; Hercules, California, USA). 80-100 μg of protein were loaded onto 4–20% Mini-PROTEAN® TGX™ Precast Gel (Biorad, 4561093EDU, USA) and transferred to polyvinylidene difluoride (PVDF) membrane (Biorad,1704272, USA) using the Trans-Blot Turbo Transfer System (BioRad, 1704150, USA). Membranes were incubated for 1hr in 5% skim milk (Biorad, 1706404, USA) prepared with 1X Tris buffered saline (TBS) (Biorad, 1706435, USA) with 0.1% Tween 20 (Sigma-Aldrich, P1379, USA). Primary antibodies were diluted in 5% Bovine serum albumin (Fisher, BP9703-100, USA) dissolved in 1X TBS. The following primary antibodies were used in the study: Mouse anti-αS (1:2000; BD Transduction Laboratories, Zymed Laboratories #610787), mouse anti-TH (1:2000; Millipore #MAB318), anti-hRXRα mouse (1:200; Abcam #ab50546). Secondary antibodies (1:10000 for all) were purchased from LI-COR: HRP goat anti-Rabbit IgG (926-80011, USA); HRP goat anti-Mouse IgG (926-80010, USA). Images of membranes were captured and analyzed using the Odyssey XF system (LI-COR, USA).

Statistical Analysis. Data were analyzed using one-way analysis of variance with Tukey post-test or Student t test using Prism (GraphPad Software 10.0.2, Inc.). Data are presented as mean ± SE.

Results

Development of PD-like mouse model associated with an increase in inflammatory response. In this study, we used an animal model of Parkinson's Disease (PD)-like pathology, as previously described by Bjorklund A et al.[20] The study involved several groups of animals: uninjected controls, and those injected with rAAV-αS, BV, AAV-GFP, and a combination of rAAV-αS and PFF (AAV/PFF). The animals were analyzed at 4- and 8-weeks post-injection. The use of AAV/PFF injections resulted in the formation of toxic α-synuclein (αS) aggregates. These inclusions were associated with increased neuronal vulnerability due to elevated cellular levels of αS at 8 weeks. **Figure 1** illustrates a significant reduction in TH^+ cells in the SNc, corresponding with a decline in DA levels at 8 weeks post-injection. Additionally, the figure highlights that TH^+ neuronal loss was more pronounced in mice injected with AAV/PFF compared to those injected with rAAV-αS without PFF ($p<0.05$), underscoring the benefits of the combined approach for accelerating the mimicry of LB-like features. Notably, no differences were observed between uninjected controls and AAV-GFP injected controls, nor between AAV-GFP and BV/αS injections (data not shown). However, substantial differences were detected between AAV-GFP and rAAV-αS as well as between AAV-GFP and AAV/PFF ($p<0.0001$).
To investigate the link between the observed TH^+ cell loss, DA deficit, and inflammation, we analyzed GFAP and Iba1 positive immunofluorescence in the injected brains. **Figure 2** demonstrates a significant increase in both GFAP and Iba1 fluorescent signals in AAV/PFF injected brains, which were previously identified with dramatic TH^+ cell loss compared to BV/αS injections (as shown in **Figure 1**). This indicates a notable inflammatory response associated with the combined AAV/PFF approach.

RXR overexpression results in a marked reduction of PD-associated pathogenesis. To explore the therapeutic potential of RXR for PD treatment, we utilized rAAV-mediated transduction to deliver either human RXRα or control GFP, alongside AAV/PFF, into the mouse SNc. Various control and experimental groups were

included in the study, incorporating combinations of GFP, human RXRα viral vectors, and control BV/αS. The mice were analyzed at 4- and 8-weeks post-injection. An unbiased stereology count of nigral TH^+ cells in the injected SNc was compared with the uninjected SNc for each mouse. No significant differences were observed between animals injected with the GFP, human RXRα vectors, and/or control BV/αS, and the uninjected side at both the 4- and 8-week time points ($p = 0.963$; data not shown). Therefore, the BV/αS control group at both time points was used for further comparisons.

Figure 3 presents the study results of the mouse SNc terminated at 4 weeks post-injection with AAV/PFF. Despite confocal imaging revealing pS129-positive aggregates in TH^+ neurons in the SNc of mice treated with AAV/PFF, no significant nigral TH^+ cell loss or marked reduction in striatal DA was detected in the mouse brain at this point (data not shown). However, a notable reduction in PPARα levels was observed in the SNc of AAV/PFF-injected mice at 4 weeks post-injection. Additionally, a significant increase in PPARα was detected in the nigral tissues injected with AAV/PFF + AAV-RXR. These findings suggest that PPAR activation is involved in the therapeutic effects mediated by RXR-based therapy.

Furthermore, RXR overexpression in mice enhances NURR1 production in the SNc at 4 weeks post-injection (**Figure 3**). This implies that RXR overexpression leads to NURR1 activation in the brain, which has been proposed as a monotherapy for PD.[19] Previous studies have shown that NURR1 activation induces TH production.[14] Consistent with this, significant upregulation of TH^+ cells and striatal DA, associated with enhanced NURR1 production at 4 weeks, was found in mouse brain tissue with AAV-mediated RXR overexpression at 8 weeks (**Figure 3**). This highlights the potential role of enhanced NURR1 in treatments involving RXR.

At 8 weeks post-injection, while AAV/PFF treatment induced a significant loss of nigral TH^+ cells and striatal DA levels (**Figure 1 and 4**), the simultaneous delivery of human RXRα resulted in a reduction of TH^+ cell loss and an increase in DA levels (**Figure 4**). Additionally, RXR overexpression led to a decrease in GFAP, indicating reduced recruitment of astrocytes to the AAV/PFF-affected area at 8 weeks post-injection (**Figure 5**). It is also noteworthy that the microglial marker Iba1 was diminished in RXR-overexpressing brains with pS129-positive aggregates, further supporting the anti-inflammatory effects of RXR overexpression.

Finally, we analyzed the distribution area of pS129-positive aggregates affected by RXR overexpression by comparing injection sites of AAV/PFF + AAV-GFP and AAV/PFF + AAV-RXR mice. We counted the pS129-positive aggregates in outlined areas (**Figure 6**). Remarkably, the number of aggregates and the size of the area containing pS129-positive aggregates, measured in μm^2, significantly decreased with the distance from the point of injection in AAV/PFF + AAV-RXR injected brains compared to AAV/PFF + AAV-GFP injections ($p<0.0001$).

Overall, our study demonstrated the therapeutic effect of RXR activation in slowing down PD progression by targeting major pathological events in the affected brains, such as the formation of LB-like structures, the loss of TH^+ neurons, and the development of an inflammatory response.

Discussion

In the current study, we proposed a reliable mouse model that mimics PD-like pathology, including the accumulation of LB-like aggregates, TH neuronal loss, and DA deficit. Our data indicate that a combination approach delivering AAV-αS and commercial PFF to the SNc results in the activation of a severe inflammatory response in the SNc by 8 weeks. This significantly accelerates PD progression compared to previously reported models based on AAV-αS injections. This confirms the observation by Bjorklund A et al. l[20] that the combined AAV/PFF delivery offers several advantages over the standard PFF model due to the enhanced and accelerated αS pathology and glial response induced by the αS-PFF and elevated αS levels, as shown in **Figure 2**. An advantage of the current study is that we demonstrated that the AAV/PFF model provides a window of opportunity for drug delivery and has been shown to be druggable, according to our data.

The AAV/PFF mouse model provides benefits by triggering an early inflammatory response observed at 4 weeks post-injection before severe aggregate formation is observed, as previously reported.[20] Notably, the significant striatal DA and nigral TH^+ cell loss was not yet detected at this time point; however, a level of protein expression induced by AAV-mediated gene transfer reaches a maximum.[23, 26, 27] These points allow to study pathogenic mechanisms triggered by AAV/PFF.

Our data indicates that overexpression of human RXRα in the SNc ameliorates αS-associated neurodegeneration. This was evident through a diminished loss of striatal DA and nigral TH+ cells, and reduced deposition of pS129-positive aggregates. Furthermore, we revealed reduced GFAP and Iba1-positive fluorescent signaling. Given the limitation of the current study, including the lack of detailed analysis of activated astrocytes and microglia phenotypes, this reduction most likely suggests fewer recruited astrocytes and Iba1-positive microglial cells, overall indicating a mitigation of neuroinflammation. In agreement with diminished neuroinflammation, the reduction in αS deposits in the PD brain also suggests that RXR upregulation most likely prohibits the aggregation of an insoluble form of the protein. The results of TH^+ cell counting, and striatal DA assay align, indicating the neuroprotective effects of RXR upregulation.

Based on our data, we anticipate that PPAR is necessary for RXR-based therapies to enhance TH cell survival and DA levels in the PD brain. We revealed that AAV/PFF treatment downregulates PPARα production. In turn, RXR overexpression induces significant upregulation of PPARα. It is well known that PPAR α, β, and γ are the permissive RXR binding partners; when activated in the central nervous system, RXR plays a critical role.[6] Recent studies have revealed reduced PPARα expression in AD brains[28] and the genetic linkage to the disease.[29, 30] The neuroprotective effect of PPAR agonists with anti-inflammatory, APP degradative, and Aβ inhibitory functions in mouse neurological models has been recently proposed.[31-35] The pharmacological modulation of PPARs by pioglitazone, rosiglitazone, ibuprofen, piroxicam, ciglitazone, and GW1929 was shown to be neuroprotective in AD, ALS, MS, and PD models.[36-41] In particular, in MPTP and 6-OHDA models of PD, preclinical studies have shown that different PPARγ agonists reduce neuronal cell death, microglial activation, and DA level in the hippocampus and the SNc.[42 16, 43 12, 44] A conformational change in the RXRa/PPARγ complex allows the heterodimer to bind PPAR-response elements (PPRE) in the nucleus to activate gene

transcription. Therefore, it is not surprising that our results have demonstrated that the AAV-mediated overexpression of human RXRα increases the expression of PPARα in mouse brains with PD-like pathology.

Our data also indicate that RXR overexpression in mice with experimental α-synucleinopathy enhances NURR1 production in SNc. This finding is in accordance with the multiple studies that highlighted the significance of NURR1 in the development of PD and related disorders. Thus, it has been shown that NURR1 is significantly decreased in the PD nigral neurons containing αS-immunoreactive inclusions and in the DA nigral neurons with neurofibrillary tangles, correlating with the loss of TH and diminished intracellular pathology in both αSNP and tauopathies.[45] Furthermore, downregulation of NURR1 promotes upregulation of the NF-κB/NLRP3 inflammasome axis,[46-48] while NURR1 overexpression and activation by means of HX600 agonist have significant anti-inflammatory effects by decreasing the expression of genes involved in inflammation control[49] and reducing microglia-expressed proinflammatory mediators, preventing neuroinflammation and neuronal cell death.[14] It is also worth mentioning that the TH upregulation and anti-inflammatory therapeutic effect from the application of HX600 agonist is associated with the activation of the NURR1/RXR complex, suggesting their dual role in PD development.

In summary, the current study not only validated a PD-like mouse model using commercially available PFF, making it convenient to study the role of genetic modifiers, but also provided evidence that mice with progressive αSNP present a model for druggable intervention in PD progression. The mechanism of RXR-based intervention requires future investigation. At this point, it is challenging to anticipate whether enhanced RXR will demonstrate a preference for binding to one nuclear receptor over another. Moreover, the RXR-based therapy may enhance the pool of RXR homodimers available to partner with both Nurr1 and PPARs to regulate the expression of genes responsible for anti-inflammatory action.

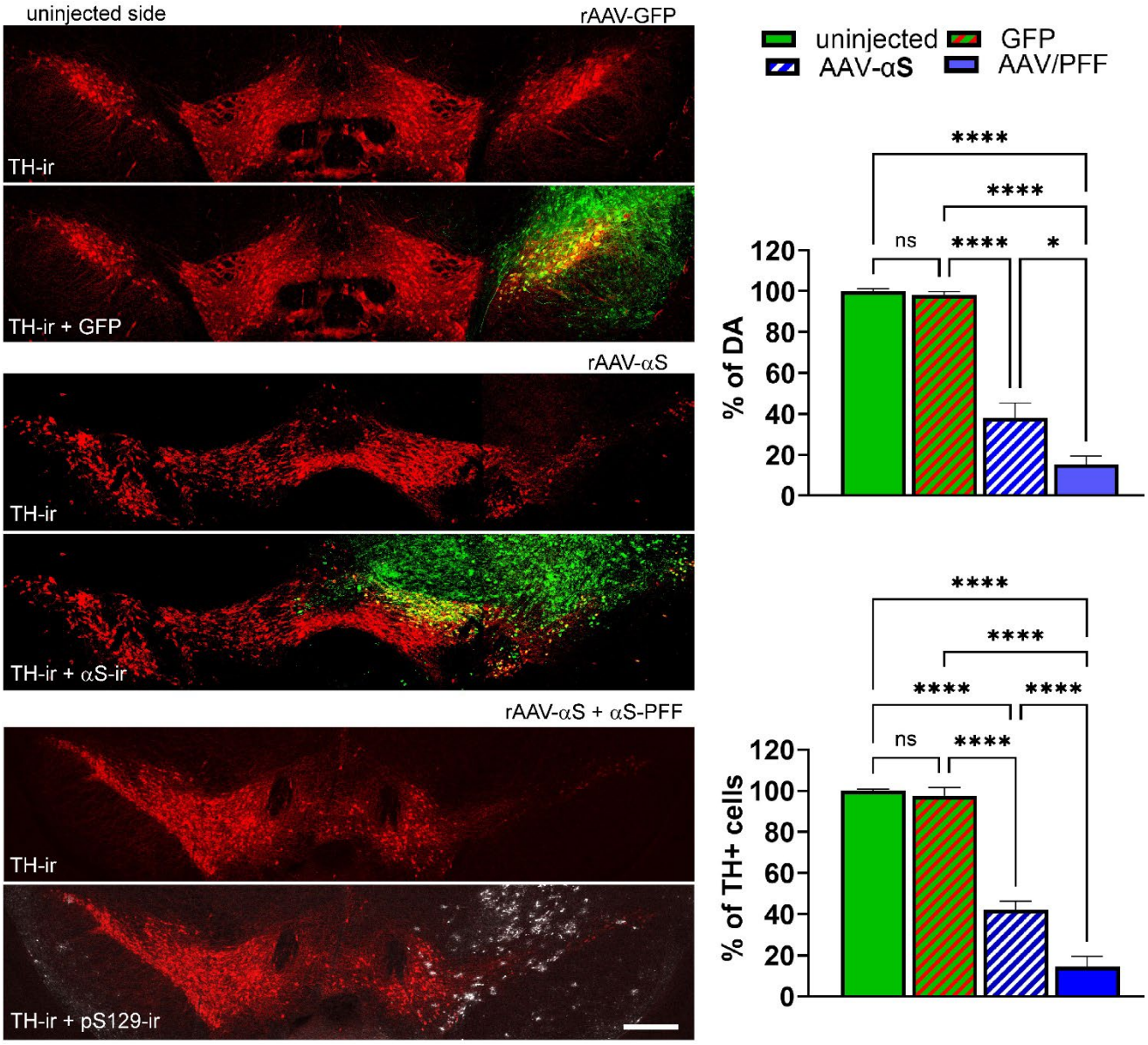

Figure 1. Comparative analysis of AAV-αS and AAV-αS /αS-PFF (AAV/PFF) mouse models of PD. All AAV vector have the same volume (0.5 µl) and titer (6 x10^{12} vg/ml). The total injection volume (1 µl) of AAV-GFP and AAV- αS was adjusted by PBS to equalize with AAV/PFF. Confocal images illustrate the PD-like pathology at 8-week post injection, which is seen as loss of TH (red) cells in the SNc and accumulation of pS129-positive (white) deposits in AAV/PFF injected brain. The graphs demonstrate the significant loss of nigral TH+ cells and striatal DA in AAV/PFF injected mice. * p< 0.05; **<0.01; ***<0.001; *** 0.0001 (n=5-6).

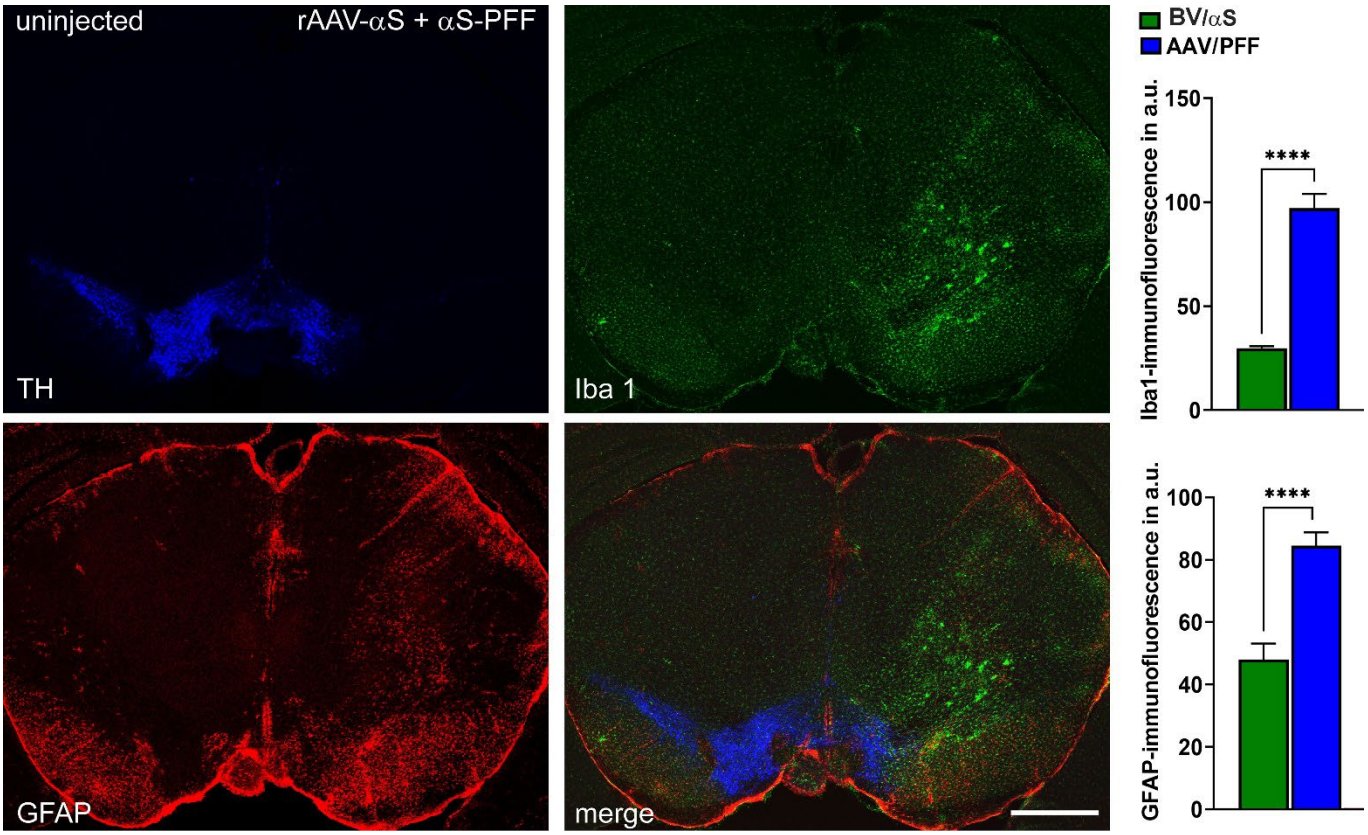

Figure 2. The mouse brain manifest increase in GFAP and Iba1, markers of astrocytes and microglia at 8-week postinjection of AAV/PFF. Of note, we did not find the difference between uninjected and injected SNc of any control groups. ***p< 0.0001 (n=4-6).

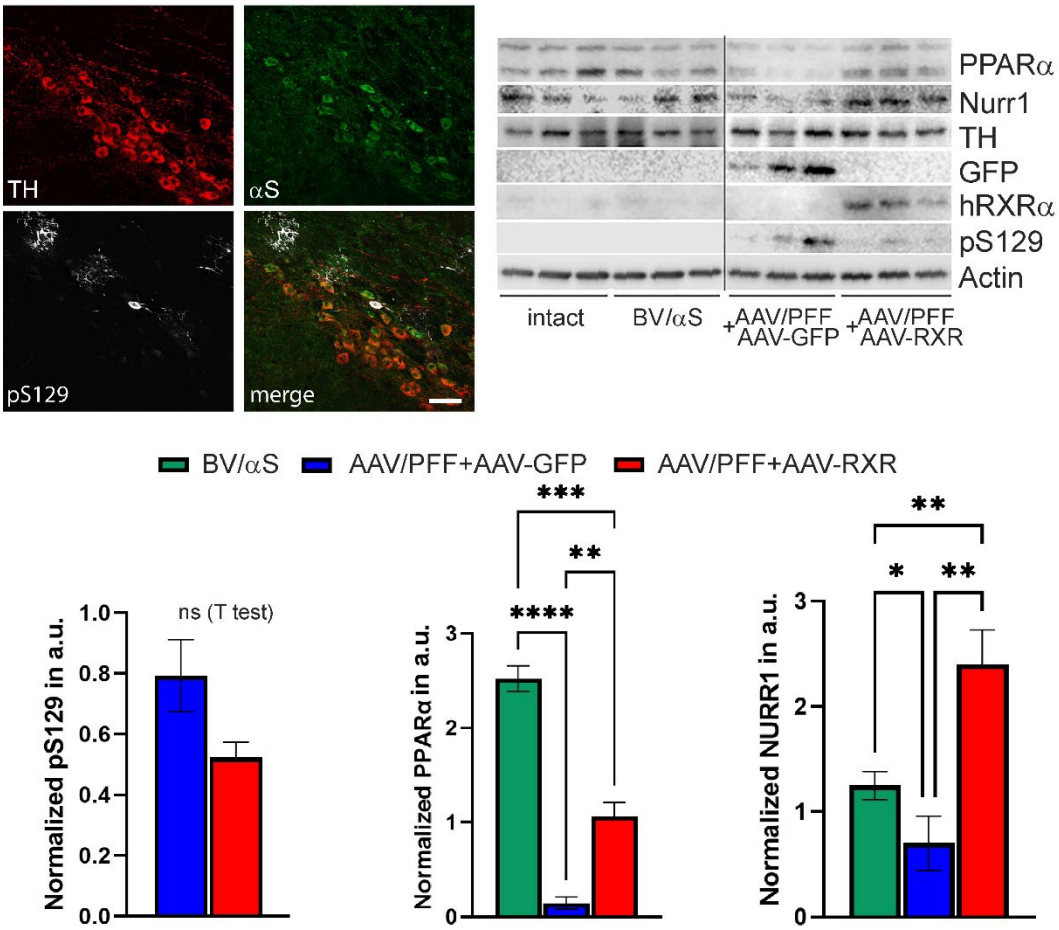

Figure 3. The SNc of mice at 4 weeks after αS-PFF and AAV vector injections. Confocal imaging reveals pS129-positive aggregates in TH+ neurons in SNc of mice treated with AAV/PFF. Western blot analyses show no difference in striatal TH protein levels between control and experimental brains, which correlates with stereology counts of TH+ cells in the SNc at this time point. Despite this, levels of PPAR and NURR1 were significantly downregulated in AAV/PFF injected brains compared to BV/αS and AAV/PFF + AAV-RXR injected brains. No difference was observed between BV/αS and uninjected brains. *p< 0.05; **<0.01 (n=6).

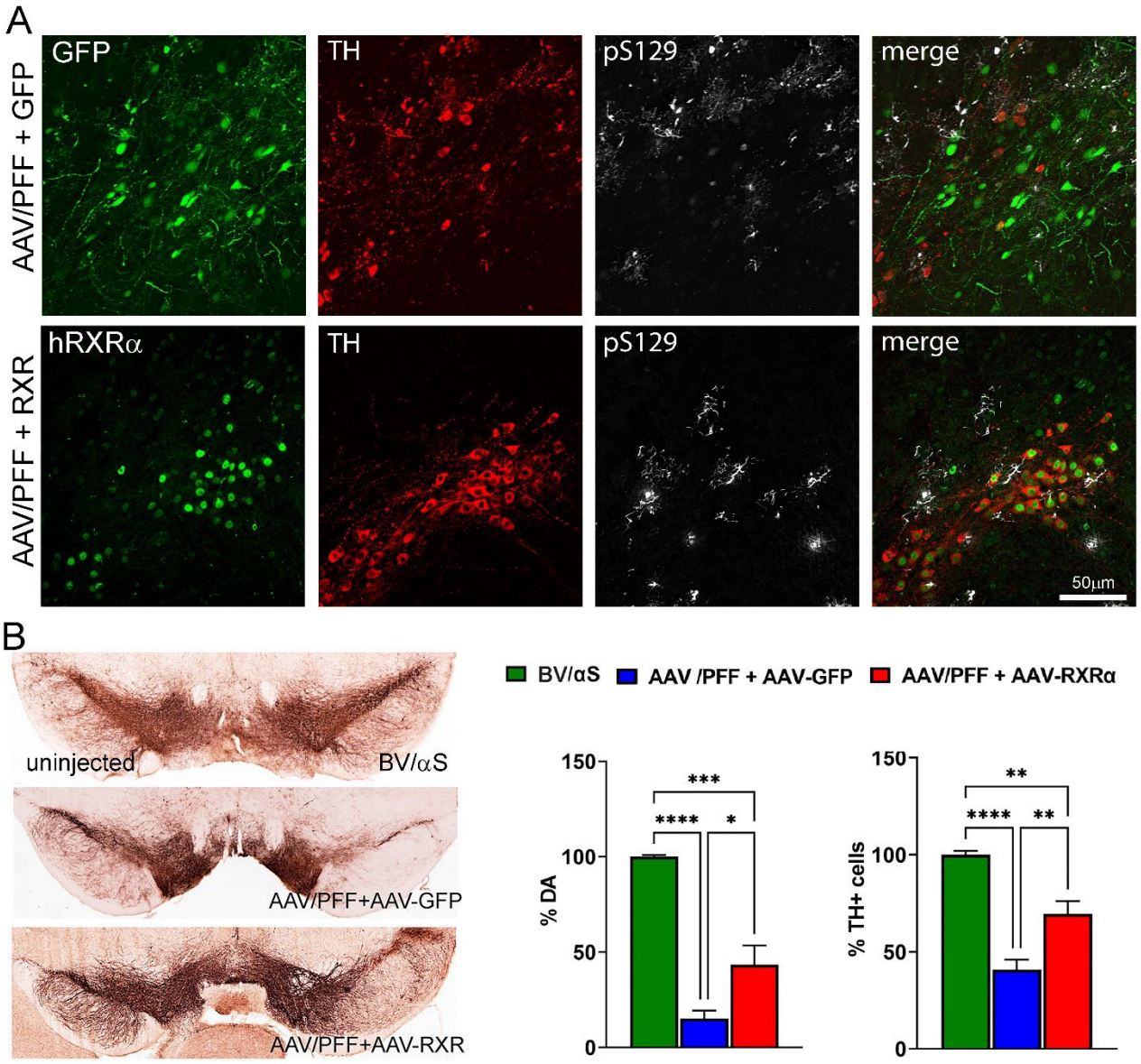

Figure 4. AAV-mediated overexpression of human (h) RXRα ameliorates PD-like pathology induced by AAV/PFF intra-nigral injection. Confocal imaging demonstrates hRXR (in green) within TH⁺ neurons (in red) with pS129 deposits (in blue). Unbiased stereology counts of TH⁺ cells and levels of striatal DA are shown. *p< 0.05; **<0.01; ***<0.001; ****<0.0001 (n=6).

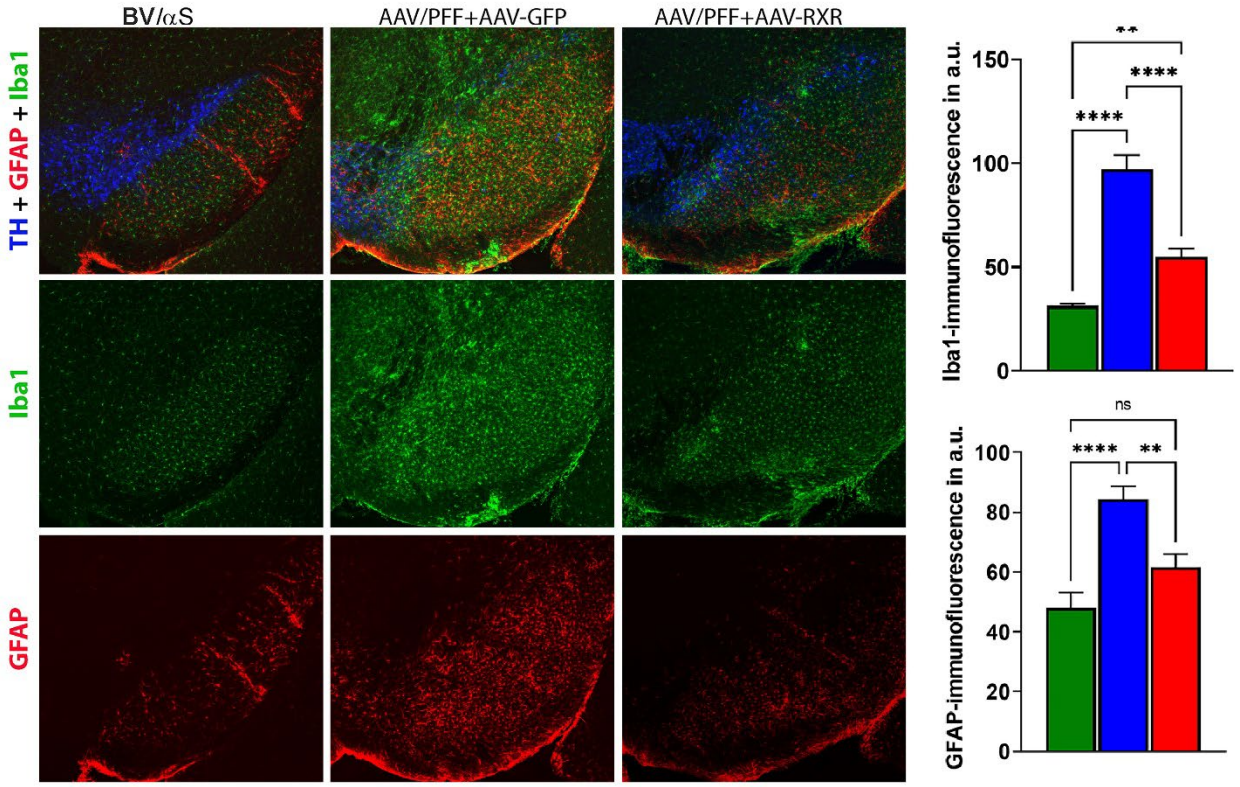

Figure 5. Confocal images illustrate reduced expression of inflammatory markers, GFAP (in red) and Iba1 (in green), in AAV/PFF brains upon AAV-RXR delivery. TH^+ cells are shown in blue. The graphs depict the results of immunofluorescent detection of GFAP and Iba1 expression shown in arbitrary units. *p< 0.05; **<0.01; ***<0.001; ****<0.0001 (n=6).

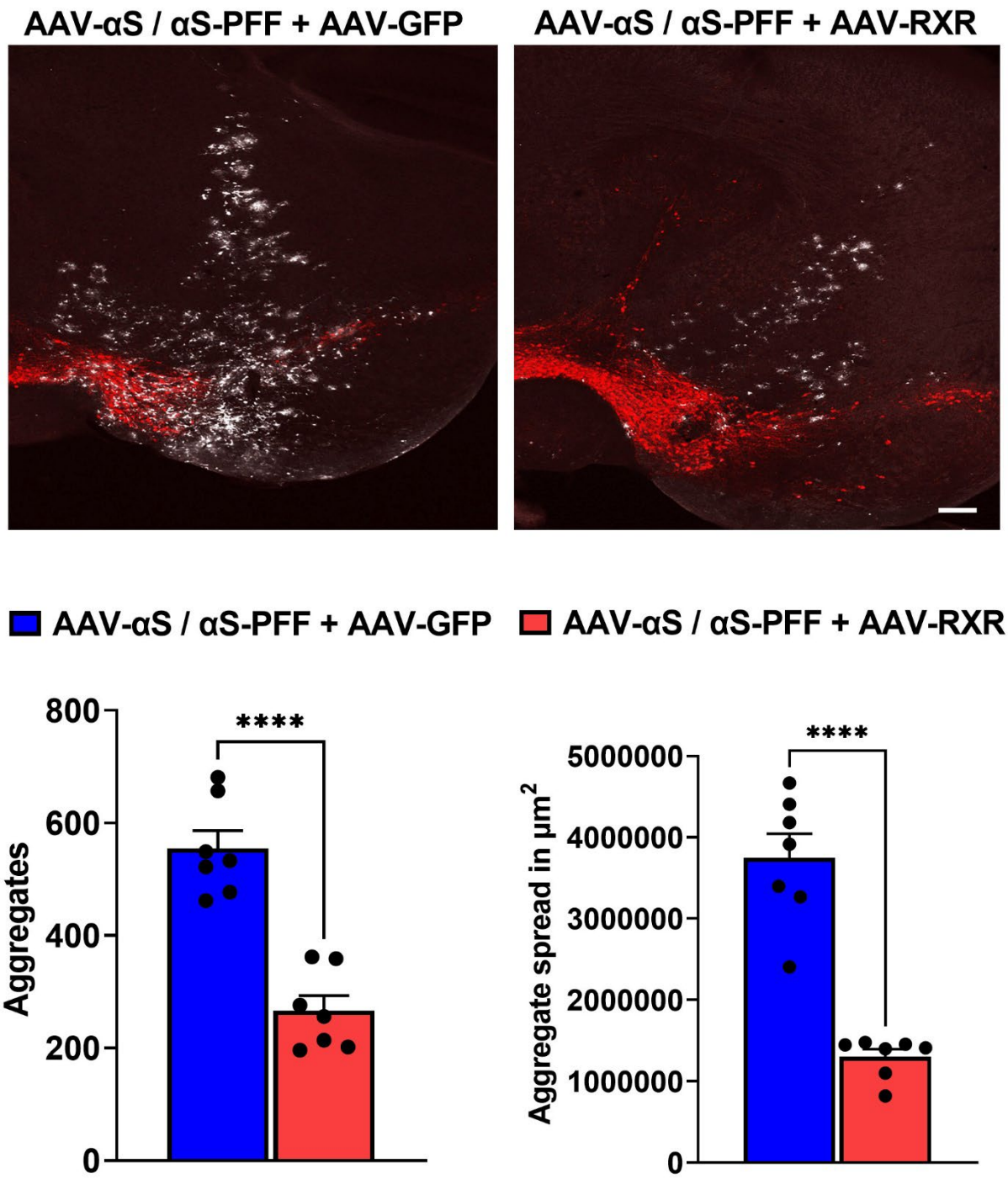

Figure 6. The pS129-positive aggregates (white) at injection sites of mouse brains treated with AAV/PFF + AAV-GFP and AAV/PFF + AAV-RXR. TH-positive cells stained in red. Graphs represent comparative count and distribution area of pS129-positive aggregates. Student t-test, ****$p<0.0001$ (n=7).

1. Wang Q, Liu Y, Zhou J. Neuroinflammation in Parkinson's disease and its potential as therapeutic target. *Transl Neurodegener* 2015;4:19.
2. Spathis AD, Asvos X, Ziavra D, et al. Nurr1:RXRalpha heterodimer activation as monotherapy for Parkinson's disease. *Proc Natl Acad Sci U S A* 2017;114:3999-4004.
3. Friling S, Bergsland M, Kjellander S. Activation of Retinoid X Receptor increases dopamine cell survival in models for Parkinson's disease. *BMC Neurosci* 2009;10:146.
4. Al-Nusaif M, Yang Y, Li S, Cheng C, Le W. The role of NURR1 in metabolic abnormalities of Parkinson's disease. *Mol Neurodegener* 2022;17:46.
5. Sharma S, Shen T, Chitranshi N, et al. Correction to: Retinoid X Receptor: Cellular and Biochemical Roles of Nuclear Receptor with a Focus on Neuropathological Involvement. *Mol Neurobiol* 2022;59:2051.
6. van Neerven S, Kampmann E, Mey J. RAR/RXR and PPAR/RXR signaling in neurological and psychiatric diseases. *Prog Neurobiol* 2008;85:433-451.
7. Corona JC, Duchen MR. PPARgamma and PGC-1alpha as therapeutic targets in Parkinson's. *Neurochem Res* 2015;40:308-316.
8. Corona JC, Duchen MR. PPARgamma as a therapeutic target to rescue mitochondrial function in neurological disease. *Free Radic Biol Med* 2016;100:153-163.
9. Rahimi A, Faizi M, Talebi F, Noorbakhsh F, Kahrizi F, Naderi N. Interaction between the protective effects of cannabidiol and palmitoylethanolamide in experimental model of multiple sclerosis in C57BL/6 mice. *Neuroscience* 2015;290:279-287.
10. Ferret-Sena V, Capela C, Sena A. Metabolic Dysfunction and Peroxisome Proliferator-Activated Receptors (PPAR) in Multiple Sclerosis. *Int J Mol Sci* 2018;19.
11. Le WD, Xu P, Jankovic J, et al. Mutations in NR4A2 associated with familial Parkinson disease. *Nat Genet* 2003;33:85-89.
12. Perez-Segura I, Santiago-Balmaseda A, Rodriguez-Hernandez LD, et al. PPARs and Their Neuroprotective Effects in Parkinson's Disease: A Novel Therapeutic Approach in alpha-Synucleinopathy? *Int J Mol Sci* 2023;24.
13. Al-Nusaif M, Lin Y, Li T, Cheng C, Le W. Advances in NURR1-Regulated Neuroinflammation Associated with Parkinson's Disease. *Int J Mol Sci* 2022;23.
14. Loppi S, Kolosowska N, Karkkainen O, et al. HX600, a synthetic agonist for RXR-Nurr1 heterodimer complex, prevents ischemia-induced neuronal damage. *Brain Behav Immun* 2018;73:670-681.
15. Wang J, Bi W, Zhao W, et al. Selective brain penetrable Nurr1 transactivator for treating Parkinson's disease. *Oncotarget* 2016;7:7469-7479.
16. Machado MMF, Bassani TB, Coppola-Segovia V, et al. PPAR-gamma agonist pioglitazone reduces microglial proliferation and NF-kappaB activation in the substantia nigra in the 6-hydroxydopamine model of Parkinson's disease. *Pharmacol Rep* 2019;71:556-564.
17. Argyrofthalmidou M, Spathis AD, Maniati M, et al. Nurr1 repression mediates cardinal features of Parkinson's disease in alpha-synuclein transgenic mice. *Hum Mol Genet* 2021;30:1469-1483.
18. Kim W, Tripathi M, Kim C, et al. An optimized Nurr1 agonist provides disease-modifying effects in Parkinson's disease models. *Nat Commun* 2023;14:4283.
19. Saijo K, Winner B, Carson CT, et al. A Nurr1/CoREST pathway in microglia and astrocytes protects dopaminergic neurons from inflammation-induced death. *Cell* 2009;137:47-59.
20. Bjorklund A, Nilsson F, Mattsson B, Hoban DB, Parmar M. A Combined alpha-Synuclein/Fibril (SynFib) Model of Parkinson-Like Synucleinopathy Targeting the Nigrostriatal Dopamine System. *J Parkinsons Dis* 2022;12:2307-2320.
21. Gully JC, Sergeyev VG, Bhootada Y, et al. Up-regulation of activating transcription factor 4 induces severe loss of dopamine nigral neurons in a rat model of Parkinson's disease. *Neurosci Lett* 2016;627:36-41.
22. Salganik M, Sergeyev VG, Shinde V, et al. The loss of glucose-regulated protein 78 (GRP78) during normal aging or from siRNA knockdown augments human alpha-synuclein (alpha-syn) toxicity to rat nigral neurons. *Neurobiol Aging* 2015;36:2213-2223.
23. Gorbatyuk MS, Shabashvili A, Chen W, et al. Glucose regulated protein 78 diminishes alpha-synuclein neurotoxicity in a rat model of Parkinson disease. *Mol Ther* 2012;20:1327-1337.
24. Maidana DE, Tsoka P, Tian B, et al. A Novel ImageJ Macro for Automated Cell Death Quantitation in the Retina. *Invest Ophthalmol Vis Sci* 2015;56:6701-6708.

25. Kirik D, Rosenblad C, Burger C, et al. Parkinson-like neurodegeneration induced by targeted overexpression of alpha-synuclein in the nigrostriatal system. *J Neurosci* 2002;22:2780-2791.
26. Burger C, Gorbatyuk OS, Velardo MJ, et al. Recombinant AAV viral vectors pseudotyped with viral capsids from serotypes 1, 2, and 5 display differential efficiency and cell tropism after delivery to different regions of the central nervous system. *Mol Ther* 2004;10:302-317.
27. Gorbatyuk OS, Li S, Nguyen FN, et al. alpha-Synuclein expression in rat substantia nigra suppresses phospholipase D2 toxicity and nigral neurodegeneration. *Mol Ther* 2010;18:1758-1768.
28. Wojtowicz S, Strosznajder AK, Jezyna M, Strosznajder JB. The Novel Role of PPAR Alpha in the Brain: Promising Target in Therapy of Alzheimer's Disease and Other Neurodegenerative Disorders. *Neurochem Res* 2020;45:972-988.
29. Koivisto AM, Helisalmi S, Pihlajamaki J, et al. Association analysis of peroxisome proliferator-activated receptor gamma polymorphisms and late onset Alzheimer's disease in the Finnish population. *Dement Geriatr Cogn Disord* 2006;22:449-453.
30. Hamilton G, Proitsi P, Jehu L, et al. Candidate gene association study of insulin signaling genes and Alzheimer's disease: evidence for SOS2, PCK1, and PPARgamma as susceptibility loci. *Am J Med Genet B Neuropsychiatr Genet* 2007;144B:508-516.
31. Heneka MT, Sastre M, Dumitrescu-Ozimek L, et al. Acute treatment with the PPARgamma agonist pioglitazone and ibuprofen reduces glial inflammation and Abeta1-42 levels in APPV717I transgenic mice. *Brain* 2005;128:1442-1453.
32. Sung B, Park S, Yu BP, Chung HY. Amelioration of age-related inflammation and oxidative stress by PPARgamma activator: suppression of NF-kappaB by 2,4-thiazolidinedione. *Exp Gerontol* 2006;41:590-599.
33. Sastre M, Dewachter I, Landreth GE, et al. Nonsteroidal anti-inflammatory drugs and peroxisome proliferator-activated receptor-gamma agonists modulate immunostimulated processing of amyloid precursor protein through regulation of beta-secretase. *J Neurosci* 2003;23:9796-9804.
34. Sastre M, Dewachter I, Rossner S, et al. Nonsteroidal anti-inflammatory drugs repress beta-secretase gene promoter activity by the activation of PPARgamma. *Proc Natl Acad Sci U S A* 2006;103:443-448.
35. Camacho IE, Serneels L, Spittaels K, Merchiers P, Dominguez D, De Strooper B. Peroxisome-proliferator-activated receptor gamma induces a clearance mechanism for the amyloid-beta peptide. *J Neurosci* 2004;24:10908-10917.
36. Chao X, Xiong C, Dong W, et al. Activation of peroxisome proliferator-activated receptor beta/delta attenuates acute ischemic stroke on middle cerebral ischemia occlusion in rats. *J Stroke Cerebrovasc Dis* 2014;23:1396-1402.
37. Kalra P, Khan H, Kaur A, Singh TG. Mechanistic Insight on Autophagy Modulated Molecular Pathways in Cerebral Ischemic Injury: From Preclinical to Clinical Perspective. *Neurochem Res* 2022;47:825-843.
38. Prashantha Kumar BR, Kumar AP, Jose JA, et al. Minutes of PPAR-gamma agonism and neuroprotection. *Neurochem Int* 2020;140:104814.
39. Tong Q, Wu L, Gao Q, Ou Z, Zhu D, Zhang Y. PPARbeta/delta Agonist Provides Neuroprotection by Suppression of IRE1alpha-Caspase-12-Mediated Endoplasmic Reticulum Stress Pathway in the Rotenone Rat Model of Parkinson's Disease. *Mol Neurobiol* 2016;53:3822-3831.
40. Falcone R, Florio TM, Di Giacomo E, et al. PPARbeta/delta and gamma in a rat model of Parkinson's disease: possible involvement in PD symptoms. *J Cell Biochem* 2015;116:844-855.
41. Lee Y, Cho JH, Lee S, et al. Neuroprotective effects of MHY908, a PPAR alpha/gamma dual agonist, in a MPTP-induced Parkinson's disease model. *Brain Res* 2019;1704:47-58.
42. Bonato JM, Bassani TB, Milani H, Vital M, de Oliveira RMW. Pioglitazone reduces mortality, prevents depressive-like behavior, and impacts hippocampal neurogenesis in the 6-OHDA model of Parkinson's disease in rats. *Exp Neurol* 2018;300:188-200.
43. Barbiero JK, Santiago RM, Persike DS, et al. Neuroprotective effects of peroxisome proliferator-activated receptor alpha and gamma agonists in model of parkinsonism induced by intranigral 1-methyl-4-phenyl-1,2,3,6-tetrahyropyridine. *Behav Brain Res* 2014;274:390-399.
44. Hassanzadeh K, Rahimmi A, Moloudi MR, et al. Effect of lobeglitazone on motor function in rat model of Parkinson's disease with diabetes co-morbidity. *Brain Res Bull* 2021;173:184-192.
45. Chu Y, Le W, Kompoliti K, Jankovic J, Mufson EJ, Kordower JH. Nurr1 in Parkinson's disease and related disorders. *J Comp Neurol* 2006;494:495-514.

46. Li T, Tan X, Tian L, et al. The role of Nurr1-miR-30e-5p-NLRP3 axis in inflammation-mediated neurodegeneration: insights from mouse models and patients' studies in Parkinson's disease. *J Neuroinflammation* 2023;20:274.
47. Li W, Liu X, Tu Y, et al. Dysfunctional Nurr1 promotes high glucose-induced Muller cell activation by up-regulating the NF-kappaB/NLRP3 inflammasome axis. *Neuropeptides* 2020;82:102057.
48. Paik S, Kim JK, Silwal P, Sasakawa C, Jo EK. An update on the regulatory mechanisms of NLRP3 inflammasome activation. *Cell Mol Immunol* 2021;18:1141-1160.
49. Briand O, Helleboid-Chapman A, Ploton M, et al. The nuclear orphan receptor Nur77 is a lipotoxicity sensor regulating glucose-induced insulin secretion in pancreatic beta-cells. *Mol Endocrinol* 2012;26:399-413.